Stereoselective Trans Addition of D_2 to the Coordinated $RN{=}C(R^1)C(H){=}NR$ Ligand in $FeRu(CO)_6$(R-DAB;R^1,H(6e)) To Afford $FeRu(CO)_6(\mu,\mu'$-$N(R)CR^1DCHDN(R))$ (R = *i*-Pr, R^1 = Me, H; R = *p*-Tol, R^1 = H). Kinetic ^1H NMR Studies of the Hydrogenation at Hydrogen Pressures between 1 and 70 bar. Single-Crystal X-ray Structure Determinations of $FeRu(CO)_6(\mu,\mu'$-$N(R)CH_2CR^1HN(R))$ (R = *i*-Pr and R^1 = H, Me)[1]

Robert Zoet, Cornelis J. Elsevier, Gerard van Koten, Peter Versloot, Kees Vrieze,* and Maarten van Wijnkoop

Anorganisch Chemisch Laboratorium, University of Amsterdam, Nieuwe Achtergracht 166, 1018 WV Amsterdam, The Netherlands

Cornelis A. Duineveld, Kees Goubitz, Dick Heijdenrijk, and Casper H. Stam

Laboratorium voor Kristallografie, University of Amsterdam, Nieuwe Achtergracht 166, 1018 WV Amsterdam, The Netherlands

Received January 13, 1988

Reaction of $FeRu(CO)_6$(R-DAB;R^1,H(6e))[1b] (**1a**, R = *i*-Pr, R^1 = H; **1b**, R = *i*-Pr, R^1 = Me; **1c**, R = *p*-Tol, R^1 = H) with molecular hydrogen at 90 °C yielded $FeRu(CO)_6(\mu,\mu'$-$N(R)CHR^1CH_2N(R))$ (**2a**, R = *i*-Pr, R^1 = H; **2b**, R = *i*-Pr, R^1 = Me; **2c**, R = *p*-Tol, R^1 = H). During the reaction the neutral, 6e-bonded R-DAB ligand is dihydrogenated to a formally dianionic, 6e-bonded bridging 1,2-ethanediyldiamido ligand, as evidenced by the single-crystal X-ray structure determinations of **2a** and **2b**. Crystals of $FeRu(CO)_6$-$(\mu,\mu'$-N(*i*-Pr)CH_2CH_2N(*i*-Pr)) (**2a**) are orthorhombic, space group $Pca2_1$, with a = 14.416 (3) Å, b = 19.242 (4) Å, c = 13.640 (3) Å, and Z = 8. The structure was solved by using direct methods and refinement converged to R = 0.068 and R_w = 0.105 using 3290 independent reflections above the $2.5\sigma(I)$ level. Crystals of $FeRu(CO)_6(\mu,\mu'$-N(*i*-Pr)CH_2CHMeN(*i*-Pr)) (**2b**) are monoclinic, space group $P2_1/n$, with a = 15.330 (4) Å, b = 26.431 (7) Å, c = 9.692 (3) Å, β = 99.52 (4)°, and Z = 8. The structure was solved by Patterson methods and was refined to R = 0.055 and R_w = 0.097 using 3750 independent reflections above the $2\sigma(I)$ level. In the unit cells of both **2a** and **2b** two independent molecules are found which have only slightly different geometries. Complex **2a** exhibits C_s symmetry and consists of a $FeRu(CO)_6$ unit (Fe–Ru = 2.452 (2) Å) to which the 1,2-ethanediylbis(isoproylamido) ligand is bonded via both nitrogen atoms in a bridging fashion. The two iron–nitrogen bonds are 2.024 (6) Å (mean), and the two ruthenium–nitrogen bonds are 2.075 (6) Å (mean). The intraligand bond lengths and angles are consistent with a reduction of both C=N bonds of the α-diimine to sp^3 C–N bonds: C(7)–N(1) and C(8)–N(2) amount to 1.48 (1) Å and C(7)–C(8) amounts to 1.57 (2) Å. Complex **2b** shows almost identical geometrical features compared to those of **2a**. The main difference is the methyl group C(15) in **2b** which is directed toward the iron atom in the molecule. Reactions of **1a** and **1b** with deuterium yielded $FeRu(CO)_6(\mu,\mu'$-N(*i*-Pr)CHDCHDN(*i*-Pr)) (**3a**) and $FeRu(CO)_6(\mu,\mu'$-N(*i*-Pr)CHDCMeDN(*i*-Pr)) (**3b**), respectively. It has been concluded from ^1H NMR studies that the deuteriation reactions result in a stereospecific trans addition over the central C—C bond of the N=CC=N skeleton of the R-DAB ligand. The reaction of **1a** with hydrogen to **2a** was monitored by ^1H NMR in a pressurizable sapphire NMR tube. These measurements showed that the reaction was very slow below a temperature of about 343 K at hydrogen pressures between 20 and 70 bar. No intermediates have been observed. The rate of the conversion of **1a** to **2a** is first-order in the concentrations of both **1a** and hydrogen. For the activation energy of the reaction of **1a** with hydrogen to **2a** an E/R of 13 (3) K was calculated.

Introduction

It has now been amply demonstrated that the versatile α-diimine ligands R-DAB and R-Pyca[1b] may utilize not only the electron pairs on one or both N atoms for coordination but also the π-C=N bonds of the imine moieties.[2a–c] A central theme of our research involves the exploration of the chemical properties of the metal–η^2-C=N bonded unit. It has been shown for reactions of in particular $M_2(CO)_6$(α-diimine) (M = Fe, Ru; α-diimine = R-DAB, R-Pyca) with suitable heteroolefins and heteroalkynes that both C–C and C–N bonds may be formed between the η^2-C=N-coordinated imine unit and the substrate.[2b,3a–f]

* To whom correspondence should be addressed.

(1) (a) Part 16. For earlier parts see ref 10. (b) 1,4-Disubstituted-1,4-diaza-1,3-dienes, RN=C(R^1)C(R^2)=NR, are abbreviated as R-DAB-{R^1,R^2}. When R^1 = R^2 = H, the abbreviation R-DAB can be used. pyridine-2-carbaldimines, C_5H_4N-2-C(H)=NR, are abbreviated as R-Pyca. The number of electrons donated by the α-dimine ligand to the cluster is indicated in parentheses: i.e. α-dimine(4e) stands for σ,σ-N,N′ chelating, 4e coordinated; α-diimine(6e) stands for σ-N, μ_2-N′, η^2-C=N′ bridging, 6e coordinated; α-diimine(8e) stands for σ,σ-N,N′, η^2,η^2-C=N,C′=H′ bridging, 8e coordinated.

(2) (a) van Koten, G.; Vrieze, K. *Adv. Organomet. Chem.* **1982**, *21*, 151. (b) Vrieze, K. *J. Organomet. Chem.* **1986**, *300*, 307. (c) Vrieze, K.; van Koten, G. *Inorg. Chim. Acta* **1985**, *100*, 79.

0276-7333/89/2308-0023$01.50/0

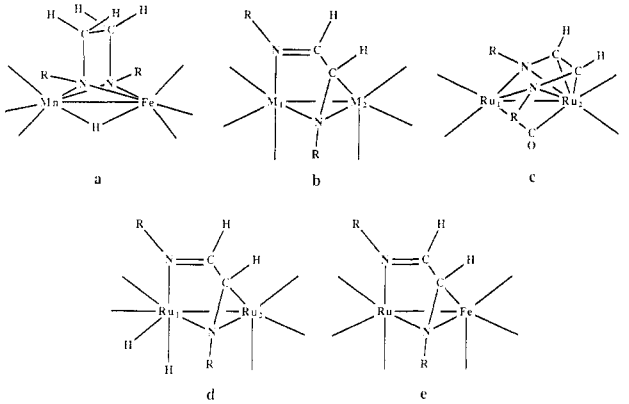

Figure 1. Schematic structures of (a) $HFeMn(\mu,\mu'\text{-}N(R)CH_2CH_2N(R))(CO)_6$, (b) $M_2(CO)_6$(R-DAB(6e)) (M = Fe, Ru), (c) $Ru_2(CO)_5$(R-DAB(8e)), (d) $H_2Ru_2(CO)_5$(R-DAB(6e)), and (e) $FeRu(CO)_6$(R-DAB(6e)).

Relatively little is known about the addition of hydrogen to the NCCN skeleton of the coordinated R-DAB ligand. It is known that the σ,σ-N,N'-coordinated R-DAB ligand in $Mn(CO)_3$(*p*-Tol-DAB(4e)) may react with $[HFe(CO)_4]^-$ to produce $HFeMn(CO)_6(\mu,\mu'\text{-}N(p\text{-Tol})CH_2CH_2N(p\text{-Tol}))$ which contains a formally dianionic diamido ligand bridging the Mn–Fe bond (Figure 1a).[4] Interestingly the use of $[DFe(CO)_4]^-$ resulted in a stereoselective trans addition of two D atoms to the two imine C atoms of the NCCN skeleton. We also attempted to prepare the coordiated diamido ligand $[RNCH_2CH_2NR]^{2-}$ by reaction of $M_2(CO)_6$(R-DAB(6e)) (M = Fe, Ru; Figure 1b) with H_2. However in the case of Fe a decomposition occurred, while for Ru first $Ru_2(CO)_5$(R-DAB(8e)) (Figure 1c) was formed to which subsequently H_2 was oxidatively added to one of the Ru atoms resulting in *cis*-$H_2Ru_2(CO)_5$(R-DAB(6e)) (Figure 1d).[5a,b] The overall reaction in the case of Ru is therefore a substitution of one CO ligand by two terminally bonded H atoms.

These findings prompted us to study the reactivity of $FeRu(CO)_6$(R-DAB(6e)) in which the R-DAB ligand is bonded in a 6e donating σ-N, μ_2-N', η^2-C=N' bonding mode to the $FeRu(CO)_6$ moiety with the imine moiety η^2-coordinated to Fe (Figure 1e). The structure of $FeRu(CO)_6$(R-DAB(6e)) is analogous to the previously studied structures of $M_2(CO)_6$(R-DAB(6e)) (M = Fe, Ru, Os) and of $MnCo(CO)_6$(*t*-Bu-DAB(6e)).[6a-d]

The study of this heterodinuclear R-DAB complexes is of interest because it is known that the presence of both Fe and Ru in $H_2FeRu_3(CO)_{13}$ is essential for the catalysis of the water-gas shift reaction.[7] Moreover, our previous work made clear that the formation of a diamido ligand from a coordinated R-DAB ligand *requires the presence of a bimetallic unit*.[4] Furthermore it was anticipated that in contrast to the relatively weak Fe–Fe bond in $Fe_2(CO)_6$(R-DAB(6e)) the Fe–Ru bond in the heterobinuclear species would sufficiently stabilize the bimetallic complex, while the presence of the Fe atom might promote hydrogenation of the imine bond in reactions with H_2.

In this paper it is shown that $FeRu(CO)_6$(R-DAB(6e)) does react with H_2 (D_2) to give $FeRu(CO)_6(\mu,\mu'\text{-}N(R)CHYCHYN(R))$ (Y = H, D) involving selective trans addition of H_2 (D_2) across the central C–C bond of the NCCN skeleton, while no loss of CO occurs.

Experimental Section

Materials and Apparatus. IR spectra were recorded with a Perkin-Elmer 283 spectrometer; FTIR spectra were obtained on a Nicolet 7199B FTIR interferometer (liquid-nitrogen-cooled Hg, Cd, Te detector). Field desorption (FD) mass spectra were obtained with a Varian MAT 711 double-focusing mass spectrometer with a combined EI/FD/FI ion source and coupled to spectro system MAT 100 data acquisition unit.[8] Elemental analyses were carried out by the section Elemental Analyses of the Institute of Applied Chemistry, TNO, Zeist, The Netherlands. NMR spectra were obtained on Bruker AC100, AC200, and WM250 spectrometers. The ^{13}C NMR spectra were recorded by using an APT pulse sequence, providing positive signals for primary and tertiary carbon atoms and negative signals for secondary and quaternary carbon atoms. NMR experiments under hydrogen pressures up to 70 bar were carried out on a Bruker AC100 using a home-built apparatus consisting of a Ti/Al/V pressure head and a 10-mm external and 8.4-mm internal diameter sapphire NMR tube, suitable for measurements under 1–140 bar of gas pressure.[9]

All synthetic preparations were carried out in an atmosphere of purified nitrogen, using carefully dried solvents. Silica gel (60 mesh) for column chromatography was activated before use. For chromatography columns of 2-cm diameter and 30-cm length were used. The $FeRu(CO)_6$(R-DAB;R^1,H(6e)) complexes (**1a**, R = *i*-Pr, R^1 = H; **1b**, R = *i*-Pr, R^1 = Me; **1c**, R = *p*-Tol, R^1 = H) were prepared according to ref 10.

Synthesis of $FeRu(CO)_6(\mu,\mu'\text{-}N(R)CHR^1CH_2N(R))$ (2a, R = *i*-Pr, R^1 = H; 2b, R = *i*-Pr, R^1 = Me; 2c, R = *p*-Tol, R^1 = H). A solution of **1a**, **1b**, or **1c** (0.5 mmol) was stirred in 100 mL of refluxing heptane while a slow hydrogen stream was passed through the solution. The reaction was continued for about 4 h until IR spectroscopy indicated that the ν(CO) pattern of the starting material had been completely replaced by that of **2a**, **2b**, or **2c**, respectively. It should be noted that below a temperature of 70 °C the rate of reaction between **1a** and hydrogen gas to give **2a** was very slow. During the reaction the color of the solution changed from red to yellow. After evaporation of the solvent the residue was dissolved in 0.5 mL of CH_2Cl_2 and was separated by column chromatography as a yellow band (eluent hexane). The eluent was concentrated to 10 mL, and upon cooling to −20 °C the product precipitated as yellow crystals. Yield: **2a**, 0.45 mmol (90%); **2b**, 0.40 mmol (80%); **2c**, 0.2 mmol (40%).

Synthesis of $FeRu(CO)_6(\mu,\mu\text{-}N(R)CDR^1CDHN(R))$ (3a, R = *i*-Pr, R^1 = H; 3b, R = *i*-Pr, R^1 = Me). A solution of **1a** and **1b** (0.5 mmol) was stirred in octane at 100 °C under an atmosphere of deuterium. The reaction was continued until IR spectroscopy indicated that the ν(CO) pattern was replaced by that of **3a** or **3b**, respectively. The purification procedure was the same as mentioned above. Yield: **3a**, 0.45 mmol (90%); **3b**, 0.40 mmol (80%).

Monitoring of the Conversion of $FeRu(CO)_6$(*i*-Pr-DAB(6e)) (1a) into $FeRu(CO)_6(\mu,\mu'\text{-}N(i\text{-Pr})CH_2CH_2N(i\text{-Pr}))$ (2a). FTIR Experiment at 1 bar of Hydrogen Pressure. The conversion of **1a** into **2a** was monitored by FTIR spectroscopy

(3) (a) Staal, L. H.; Polm, L.H.; Balk, R. W.; van Koten, G.; Vrieze, K.; Brouwers, A. M. F. *Inorg. Chem.* **1980**, *19*, 3343. (b) Muller, F.; van Koten, G.; Vrieze, K., to be submitted for publication. (c) Keijsper, J.; Polm, L.; van Koten, G.; Vrieze, K. *Inorg. Chem.* **1984**, *23*, 2142. (d) Keijsper, J.; Polm, L. H.; van Koten, G.; Schagen, J. D.; Stam, C. H.; Vrieze, K. *Inorg. Chim. Acta* **1985**, *103*, 137. (e) Keijsper, J.; Mul, J.; van Koten, G.; Vrieze, K.; Ubbels, H. C.; Stam, C. H. *Organometallics* **1984**, *3*, 1732. (f) Keijsper, J.; van Koten, G.; Vrieze, K.; Zoutberg, M.; Stam, C. H. *Organometallics* **1985**, *4*, 1306.

(4) Keijsper, J.; Grimbergen, P.; Cristophersen, M.; Stam, C. H.; van Koten, G.; Vrieze, K. *Inorg. Chim. Acta* **1985**, *102*, 29.

(5) (a) Keijsper, J.; Polm, L. H.; van Koten, G.; Nielsen, E.; Vrieze, K.; Stam, C. H. *Organometallics* **1985**, *4*, 2006. (b) Zoet, R.; Frühauf, H. W.; van Koten, G.; Vrieze, K., unpublished results.

(6) (a) Frühauf, H. W.; Landers, A.; Goddard, R.; Krüger, C. *Angew. Chem.* **1978** *90*, 56. (b) Staal, L. H.; van Koten, G.; Vrieze, K. *J. Organomet. Chem.* **1981**, *206*, 99. (c) Staal, L. H.; Keijsper, J.; van Koten, G.; Vrieze, K.; Cras, J. A.; Bosman, W. P. *Inorg. Chem.* **1981**, *20*, 555. (d) Staal, L. H.; Polm, L. H.; Balk, R. W.; van Koten, G.; Vrieze, K.; Brouwers, A. M. F. *Inorg. Chem.* **1980**, *19*, 3343.

(7) Ungermann, C.; Landis, V.; Moya, S. A.; Cohen, H.; Walker, H.; Pearson, R. G.; Ford, P. C. *J. Amer. Chem. Soc.* **1979**, *101*, 5922.

(8) Staal, L. H.; van Koten, G.; Fokkens, R. H.; Nibbering, N. M. M. *Inorg. Chim. Acta* **1981**, *50*, 205.

(9) Roe, D. C. *J. Magn. Reson.* **1985**, *63*, 388.

(10) Zoet, R.; van Koten, G.; Vrieze, K.; van Wijnkoop, M.; Goubitz, K.; van Halen, C. J. G.; Stam, C. H. *Inorg. Chim. Acta* **1988**, *149*, 193.

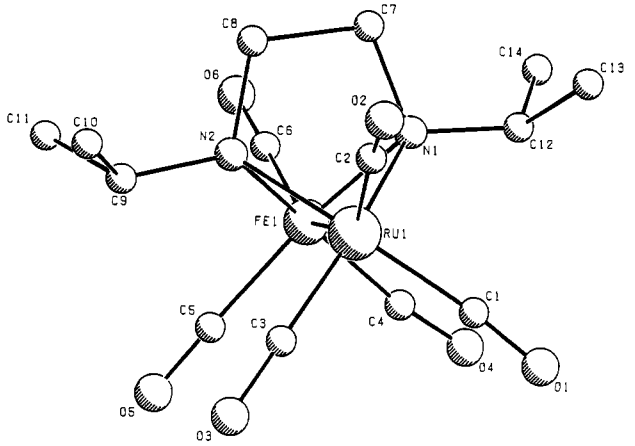

Figure 2. The molecular geometry of FeRu(μ,μ'-N(*i*-Pr)-CH_2CH_2N(*i*-Pr))$(CO)_6$ (**2a**).

by taking samples (by syringe) every 30 min of a refluxing solution of **1a** (0.5 mmol) in 100 mL of heptane.

NMR Experiments under Hydrogen Pressure. Solutions for NMR experiments under pressure were obtained by dissolving a weighed amount of crystalline material of the reactant in 1.5 mL of degassed deuteriated solvent (C_6D_6 and CD_2Cl_2). The solution was syringed into the sapphire tube, which was kept under an atmosphere of dinitrogen by using an especially designed glass vessel. Subsequently the tube was connected with a high-pressure system equipped with an accurate manometer ($\Delta P = \pm 0.5$ bar), flushed three times with hydrogen gas, and pressurized with hydrogen gas for a half an hour. Since the complexes dissolved entirely, the concentration of free hydrogen in solution could be calculated by comparing the integrated ^1H NMR intensities of the dissolved complex and hydrogen. During the monitoring of the reaction the free hydrogen concentration in solution was constant, as shown by ^1H NMR. This was accomplished by the presence of a large excess of hydrogen in the gas phase and diffusion of hydrogen gas from the gas phase into the solution during the reaction which was fast compared to the rate of the reaction. The constant free hydrogen concentration in solution implemented pseudo-first-order conditions for the kinetics of the reaction of FeRu$(CO)_6$(*i*-Pr-DAB(6e)) (**1a**) with hydrogen.

(i) Intermediates. In a search for intermediates a 0.05 M solution of **1a** in benzene-d_6 (1.5 mL) was pressurized with hydrogen gas to 20 and 70 bar, respectively, in a sapphire NMR tube (see above). ^1H NMR spectra (between 15 and −30 ppm relative to TMS) were recorded at probe temperature (300 K). Subsequently the temperature was raised from 300 to 362 K in steps of 2 K, and spectra were recorded 10 min after the new temperature had been reached.

(ii) Reaction Kinetics. A 0.05 M solution of **1a** in dichloromethane-d_2 (1.5 mL) was pressurized with hydrogen gas in a pressuriazble sapphire NMR tube to 20, 40, and 60 bar, respectively. The NMR tube was heated to 373 K, and a ^1H NMR spectrum was recorded in order to determine the concentration of free hydrogen in solution. Alternatively 0.1 M solution of **1a** in dichloromethane-d_2 (1.5 mL) was pressurized with hydrogen gas to 60 atm, and the NMR tube was heated to 383 and 393 K, respectively. Subsequently spectra were recorded every 5 min (64 scans with an a total acquisition time of 174 s; 2.72 s/scan).[11] The degree of conversion of **1a** to **2a** was studied by monitoring the decrease of the integral of the imine proton at 7.8 ppm of **1a**. The data were analyzed according to the standard first-order rate law, and linear regression analyses were used to obtain the first-order rate constant k_{obsd}.

Crystal Structure Determination of [FeRu$(CO)_6$(μ,μ'-N-(*i*-Pr)CH_2CH_2N(*i*-Pr))] (2a, $C_{14}H_{18}FeRuN_2O_6$, (1,2-Ethanediylbis(isopropylamido))hexacarbonyl-ironruthenium). Crystals of the title compound are orthorhombic, space group $Pca2_1$, with eight molecules in a unit cell of dimensions: a = 14.416 (3) Å, b = 19.242 (4) Å, c = 13.640 (3) Å, and d(calcd) = 1.64 g/cm^3. A total of 5686 independent reflections were measured on a Nonius CAD 4 diffractometer using graphite-monochromated Mo Kα radiation ($1.1 < \theta < 30°$) of which 2396 had intensities below the $2.5\sigma(I)$ level and were treated as unobserved. The metal positions were derived with direct methods using SIMPEL83.[12a] A subsequent F_o synthesis revealed the remaining non-hydrogen atoms. After isotropic block-diagonal least-squares refinement an empirical absorption correction (DIFABS) was applied (μ = 15.8 cm^{-1}).[12b] Subsequent anisotropic refinement of the non-hydrogen atoms and positional refinement of the hydrogen atoms (U fixed at 0.045 Å^2) converged to R = 0.068 and R_w = 0.105 for the 3290 observed reflections. The anomalous dispersion of iron and ruthenium was taken into account and a weighting scheme $\omega = 1/(4.1 + F_o + 0.04R_o^2)$ was applied.[12c] The computer programs used were from the XRAY76 system.[12d] The molecular geometry of **2a** with the numbering of the atoms is given in Figure 2, which shows a PLUTO drawing of the molecule.[12e] Atomic parameters, selected bond lengths, and bond angles of one molecule are given in Tables I, II, and III, respectively. A stereo ORTEP drawing, the anisotropic thermal parameters, complete listings of the atomic parameters and the bond lengths and angles of both molecules and the hydrogen

Table I. Fractional Coordinates of the Non-Hydrogen Atoms and Equivalent Isotropic Thermal Parameters of FeRu(μ,μ'-N(*i*-Pr)CH_2CH_2N(*i*-Pr))$(CO)_6$ (2a)

atom	x	y	z	U_{eq}, Å^2
Ru1	0.46292 (10)	0.12137 (7)	0.1398 (1)	0.0479 (7)
Fe1	0.45569 (10)	0.12478 (9)	0.3193 (1)	0.0228 (7)
C1	0.509 (1)	0.0332 (10)	0.110 (1)	0.06 (1)
C2	0.398 (1)	0.142 (1)	0.023 (1)	0.06 (1)
C3	0.574 (2)	0.161 (1)	0.108 (2)	0.07 (1)
C4	0.508 (1)	0.042 (1)	0.359 (2)	0.06 (1)
C5	0.566 (1)	0.166 (1)	0.361 (1)	0.06 (1)
C6	0.393 (1)	0.144 (1)	0.437 (2)	0.06 (1)
C7	0.2757 (9)	0.1290 (7)	0.224 (1)	0.043 (7)
C8	0.313 (1)	0.2059 (9)	0.224 (2)	0.052 (9)
C9	0.460 (1)	0.2730 (9)	0.228 (2)	0.055 (9)
C10	0.440 (2)	0.314 (1)	0.145 (2)	0.07 (1)
C11	0.433 (2)	0.313 (1)	0.329 (2)	0.07 (1)
C13	0.283 (2)	−0.014 (1)	0.135 (3)	0.10 (2)
C14	0.274 (2)	−0.009 (1)	0.312 (3)	0.11 (2)
N1	0.3582 (7)	0.0838 (6)	0.230 (1)	0.035 (5)
N2	0.4156 (8)	0.2020 (6)	0.2275 (10)	0.037 (6)
O1	0.5429 (9)	−0.0183 (7)	0.094 (1)	0.070 (9)
O2	0.365 (1)	0.151 (1)	−0.048 (1)	0.10 (1)
O3	0.651 (1)	0.1863 (9)	0.091 (2)	0.11 (1)
O4	0.529 (1)	−0.0130 (10)	0.379 (2)	0.10 (1)
O5	0.6339 (9)	0.191 (1)	0.384 (1)	0.09 (1)
O6	0.350 (1)	0.159 (1)	0.505 (1)	0.10 (1)

Table II. Selected Bond Lengths (Å) of the Non-Hydrogen Atoms and the Standard Deviations in Parentheses of FeRu(μ,μ'-N(*i*-Pr)CH_2CH_2N(*i*-Pr))$(CO)_6$ (2a)

Ru1–Fe1	2.452 (2)	Fe1–N2	2.027 (9)
Ru1–N1	2.077 (8)	C7–C8	1.57 (2)
Ru1–N2	2.074 (9)	C7–N1	1.48 (1)
Fe1–N1	2.020 (8)	C8–N2	1.48 (1)

Table III. Selected Bond Angles (deg) of the Non-Hydrogen Atoms with Standard Deviations in Parentheses of FeRu(μ,μ'-N(*i*-Pr)CH_2CH_2N(*i*-Pr))$(CO)_6$ (2a)

N1–Ru1–N2	71.3 (5)	Ru1–N1–C7	110.3 (8)
N1–Fe1–N2	73.5 (5)	Fe1–N1–C7	111.4 (8)
C8–C7–N1	106 (1)	Ru1–N2–Fe1	73.4 (5)
C7–C8–N2	107 (1)	Ru1–N2–C8	110.3 (9)
Ru1–N1–Fe1	73.5 (5)	Fe1–N2–C8	110.0 (9)

(11) A T_1 value of 1.13 s was measured for H_2 at 373 K in dichloromethane-d_2.

(12) (a) Schenk, H.; Kiers, C. T. SIMPEL83 In *Crystallographic Computing*; Sheldrick, G. M., Krüger, C., Goddard, R., Eds.; Clarendon: Oxford, 1985; Vol. 3. (b) Walker, N.; Stuart, D. *Acta Crystallogr.* **1983**, *A39*, 158. (c) *International Tables for Crystallography*; Kynoch: Birmingham, England 1974; Vol. IV. (d) Stewart, J. M. *The X-RAY76 System*, Technical Report TR 446; Computer Science Center: University of Maryland, College Park, MD. (e) Motherwell, S.; Glegg, G. PLUTO, Program for Plotting Molecular and Crystal Structures; University of Cambridge: Cambridge, England, 1978.

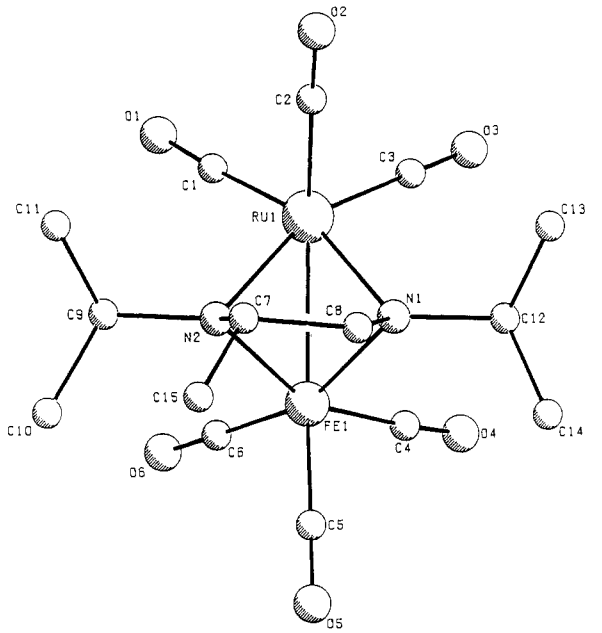

Figure 3. The molecular geometry of FeRu(μ,μ'-N(i-Pr)-CHMeCH$_2$N(i-Pr))(CO)$_6$ (**2b**).

Table IV. Fractional Coordinates of the Non-Hydrogen Atoms and Equivalent Isotropic Thermal Parameters of FeRu(μ,μ'-N(i-Pr)CHMeCH$_2$N(i-Pr))(CO)$_6$ (2b)

atom	x	y	z	U_{eq}, Å^2
Ru1	0.13132 (8)	0.22444 (5)	0.17675 (12)	0.0369 (6)
Fe1	−0.01897 (14)	0.18753 (8)	0.12514 (20)	0.0345 (11)
C1	0.2105 (12)	0.1793 (7)	0.1157 (18)	0.053 (10)
C2	0.2038 (11)	0.2825 (7)	0.1747 (18)	0.051 (10)
C3	0.1784 (11)	0.2050 (7)	0.3613 (18)	0.051 (10)
C4	−0.0244 (10)	0.1564 (6)	0.2874 (16)	0.040 (9)
C5	−0.1348 (12)	0.1934 (7)	0.0664 (18)	0.055 (11)
C6	−0.0064 (12)	0.1300 (7)	0.0435 (18)	0.053 (11)
C7	0.0043 (11)	0.2808 (6)	−0.0274 (17)	0.049 (9)
C8	−0.0202 (11)	0.2961 (6)	0.1145 (16)	0.045 (9)
C9	0.0649 (12)	0.2052 (7)	−0.1414 (18)	0.051 (10)
C10	−0.0136 (14)	0.1866 (8)	−0.2499 (21)	0.067 (13)
C11	0.1274 (13)	0.2388 (7)	−0.2050 (20)	0.057 (11)
C12	0.0007 (10)	0.2667 (6)	0.3621 (16)	0.042 (9)
C13	0.0518 (13)	0.3135 (8)	0.4222 (20)	0.063 (12)
C14	−0.0973 (15)	0.2749 (8)	0.3680 (23)	0.070 (13)
C15	−0.0733 (15)	0.2908 (8)	−0.1408 (24)	0.079 (15)
N1	0.0145 (8)	0.2559 (5)	0.2159 (12)	0.037 (7)
N2	0.0387 (8)	0.2285 (4)	−0.0081 (12)	0.037 (7)
O1	0.2635 (10)	0.1520 (6)	0.0824 (15)	0.079 (10)
O2	0.2468 (11)	0.3191 (6)	0.1772 (16)	0.090 (11)
O3	0.2062 (10)	0.1925 (5)	0.4756 (14)	0.075 (9)
O4	−0.0202 (9)	0.1340 (5)	0.3872 (14)	0.068 (9)
O5	−0.2103 (10)	0.1967 (6)	0.0262 (16)	0.084 (10)
O6	0.0066 (11)	0.0884 (6)	0.0044 (17)	0.090 (12)

atoms, and a list of observed structure factor amplitudes are included within the supplementary material.

Crystal Structure Determination of [Fe(Ru(CO)$_6$(μ,μ'-N-(i-Pr)CH$_2$CMeHN(i-Pr))] (2b, C$_{15}$H$_{20}$FeRuN$_2$O$_6$, (1,2-Propanediylbis(isopropylamido))hexacarbonylironruthenium). Crystals of the title compound are monoclinic, space group $P2_1/n$, with eight molecules in a unit cell of dimensions: a = 15.330 (4) Å, b = 26.431 (7) Å, c = 9.692 (3) Å, β = 99.52 (4)°, and d(calcd) = 1.66 g/cm^3. A total of 6947 independent reflections were measured on a Nonius CAD 4 diffractometer using graphite-monochromated Mo Kα radiation ($1.1 < \theta < 25°$) of which 3197 had intensities below the $2\sigma(I)$ level and were treated as unobserved. The metal positions were derived from an E^2 Patterson synthesis. A subsequent F_o synthesis revealed the remaining non-hydrogen atoms. After isotropic block-diagnoal least-squares refinement an empirical absorption correction (DIFABS) was applied (μ = 14.2 cm^{-1}).[12b] Subsequent anisotropic refinement with the hydrogen atoms fixed at their calculated positions converged to R = 0.055 and R_w = 0.097 for the 3750 observed reflections. The anomalous dispersion of osmium was taken into account and a weighting scheme $\omega = 1/(4.1 + F_o + 0.04F_o^2)$ was applied.[12c] The computer programs used were from the XRAY76 system.[12d] The molecular geometry of **2b** with the number of the atoms is given in Figure 3, which shows a PLUTO drawing of the molecule.[12e] Atomic parameters, selective bond lengths and bond angles of one molecule are given in Tables IV, V, and VI, respectively. A stereo ORTEP drawing, the anisotropic thermal parameters, complete listings of the atomic parameters and the bond lengths and angles of both molecules and the hydrogen atoms, and a list of observed structure amplitudes are included within the supplementary material.

Table V. Selected Bond Lengths (Å) of the Non-Hydrogen Atoms and the Standard Deviations in Parentheses of FeRu(μ,μ'-N(i-Pr)CHMeCH$_2$N(i-Pr))(CO)$_6$ (2b)

Ru1–Fe1	2.476 (2)	C7–C8	1.54 (2)
Ru1–N1	2.065 (9)	C7–C15	1.50 (2)
Ru1–N2	2.097 (8)	C7–N2	1.48 (1)
Fe1–N1	2.038 (9)	C8–N1	1.48 (1)
Fe1–N2	2.000 (8)		

Table VI. Selected Bond Angles (deg) of the Non-Hydrogen Atoms with Standard Deviations in Parentheses of FeRu(μ,μ'-N(i-Pr)CHMeCH$_2$N(i-Pr))(CO)$_6$ (2b)

N1–Ru1–N2	69.6 (5)	Ru1–N1–C8	113.2 (8)
N1–Fe1–N2	72.0 (5)	Fe1–N1–C8	108.2 (8)
C8–C7–C15	109 (1)	Ru1–N2–Fe1	74.3 (5)
C8–C7–N2	105 (1)	Ru1–N2–C7	109.4 (8)
C15–C7–N2	119 (1)	Ru1–N2–C9	117.4 (8)
C7–C8–N1	107 (1)	Fe1–N2–C7	113.6 (8)
Ru–N1–Fe1	74.2 (5)		

Table VII. IR and FD-MS Data

compd	M,[a] m/z	IR[b]
2a	468 (468)	2067, 2026, 1987, 1978, 1959
2b	482 (482)	2063, 2023, 1986, 1977, 1958
2c	564 (564)	2069, 2028, 1997, 1980, 1961
3a	470 (470)	2067, 2026, 1987, 1978, 1959
3b	484 (484)	2063, 2023, 1986, 1977, 1958

[a] The observed and calculated (in parentheses) masses account for the highest peak of the observed and simulated spectra. [b] In n-hexane, ν(CO), cm^{-1}.

Scheme I. Schematic Representation of the Reaction of FeRu(CO)$_6$(R-DAB(6e)) (1) with Molecular Hydrogen to FeRu(μ,μ'-N(R)CH$_2$CH$_2$N(R))(CO)$_6$ (2)

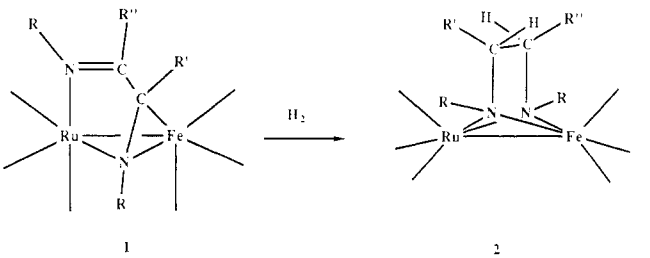

1 2

Analytical and Spectroscopic Data. Elemental analysis of all compounds gave satisfactory results (supplementary material). The complexes showed characteristic ν(CO) IR absorptions which are listed in Table VII. FD-mS spectra were recorded for all compounds. The spectra showed a FeRu isotopic pattern around the m/z value of the molecular ion that is in agreement with simulated spectra (Table VII).

Results

Formation of Products. Complexes **2** are formed according to the reaction in Scheme I.

Reaction of FeRu(CO)$_6$(R-DAB;R^1,H(6e))[1b] (**1a**, R = i-Pr, R^1 = H; **1b**, R = i-Pr, R^1 = Me; **1c**, R = p-Tol, R^1 = H) with molecular hydrogen in refluxing heptane yielded virtually quantitatively FeRu(CO)$_6$(μ,μ'-N(R)CHR^{1}CH$_2$N-

Table VIII. ^{1}H NMR Data[a]

compd	chemical shifts[b] R group	ethane	$C9H_3$
2a[c]	0.98 (d, 7 Hz, 6 H)/1.02 (d, 7 Hz, 6 H) 3.12 (sept, 7 Hz, 2 H)	H1 to H4: 2.42 (m, 4 H)	
2b[d]	0.90 (d, 6 Hz, 3 H)/1.00 (d, 6 Hz, 3 H) 1.09 (d, 6 Hz, 3 H)/1.10 (d, 6 Hz, 3 H) 3.09 (m, 2 H); 3.32 (sept, 6 Hz, 1 H)	H1: 2.64 (dd, 11 Hz, 7 Hz, 1 H) H2: 2.07 (dd, 11 Hz, 5 Hz, 1 H) H3: 3.09 (m, 2 H)	0.72 (d, 6 Hz, 3 H)
2c[d]	1.98 (s, 6 H); 6.79 (d, 8 Hz, 4 H); 7.17 (d, 8 Hz, 4 H)	H1 to H4: 2.86 (m, 4 H)	
3a[d]	0.95 (d, 7 Hz, 6 H)/1.00 (d, 7 Hz, 6 H) 3.11 (sept, 7 Hz, 2 H)	H2,H4: 2.32 (d, 3 Hz, 1 H) 2.41 (d, 3 Hz, 1 H)	
3b[c]	0.90 (d, 6 Hz, 3 H)/1.04 (d, 6 Hz, 3 H) 1.08 (d, 6 Hz, 3 H)/1.11 (d, 6 Hz, 3 H) 3.07 (sept, 6 Hz, 1 H); 3.33 (sept, 6 Hz, 1 H)	H2: 2.61 (s, 1 H)	0.72 (s, 3 H)

[a] The values (ppm relative to TMS) have been obtained in benzene-d_6 solutions. Vertical bars separate diastereotopic pairs. Abbreviations: s, singlet; d, doublet; dd, doublet of doublets; sept, septet; m, multiplet. [b] Indices according to Figures 4 and 5. [c] Obtained at 200 MHz. [d] Obtained at 250 MHz.

(R)) (**2a**, R = *i*-Pr, R^1 = H; **2b**, R = *i*-Pr, R^1 = Me; **2c**, R = *p*-Tol, R^1 = H). In the course of the reaction the neutral 6e bonded R-DAB ligand is reduced to a formally dianionic, 6e bonded bridging ethanediyldiamido ligand, as evidenced by single-crystal X-ray structure determinations of **2a** and **2b** (vide infra). It is important to note that in the case of **2b** the methyl group (R^1) is directed to the iron atom in the molecule.

Reaction of **1a** and **1b** with deuterium gas yielded $FeRu(CO)_6(\mu,\mu$-N(*i*-Pr)CHDCHDN(*i*-Pr)) (**3a**) and $FeRu(CO)_6(\mu,\mu'$-N(*i*-Pr)CHDCMeDN(*i*-Pr)) (**3b**), respectively. NMR spectroscopy revaled that the D atoms are in mutual trans positions on the adjacent carbon atoms.

Before considering the possible reaction mechanisms for the formation of the complexes in more detail, the molecular structures of **2a** and **2b**, the NMR data, and the kinetics of the reaction will be discussed.

Molecular Geometries of $FeRu(CO)_6(\mu,\mu'$-N(*i*-Pr)-CH_2CMeHN(*i*-Pr)) (2b). The molecular geometry of **2a** together with the atomic numbering is given in Figure 2. In Tables II and III selected bond lengths and angles are given. The molecular geometry of **2b**, which is in many respects similar to that of **2a** (see below), is depicted in Figure 3. Selected bond lengths and angles for **2b** are given in Tables V and VI, respectively. The crystals of both **2a** and **2b** contain two independent molecules in the unit cell which have only slightly different geometries of which only one of the independent molecules will be discussed (see tables). Since **2a** and **2b** show identical geometrical features, we will first discuss **2a** and take note of the structural differences that **2b** shows with respect to **2a**.

Molecular Geometry of 2a. As depicted in Figure 2 **2a** possesses (noncrystallographic) C_s symmetry and has a mirror plane through the midpoint of the C(7)–C(8) bond and the Fe and Ru atoms. The metal carbonyl part has the normal "sawhorse" structure with an eclipsed $(CO)_3$-$FeRu(CO)_3$ configuration [Fe–C(O) = 1.86 (1) Å (mean) and Ru–C(O) = 1.86 (1) Å (mean)]. The bite angles of N(1)–Fe–N(2) of 73.5 (5)° and N(1)–Ru–N(2) of 71.3 (5)° have normal values for dinitrogen ligand bridged species, for example, $[NHFe(CO)_3]_2$.[13] The Fe–Ru bond length of 2.452 (2) Å is rather short when compared to other FeRu complexes. For example in complex **1a**, containing a bridging 6e donating R-DAB ligand, the Fe–Ru bond is 2.6602 (9) Å.[10] In other FeRu species the Fe–Ru bond length may vary between 2.56 and 2.76 Å.[14a,b] The short Fe–Ru bond lengths in complex **2a** could be due to the rigidity of the diamido ligand with M–N–M angles of about 74°.[13,15] In $(\mu$-H)$FeMn(CO)_6(\mu,\mu'$-N(*p*-Tol)CH_2CH_2N(*p*-Tol)), which also contains a bridging ethanediyldiamido ligand similar to that of **2a**, a very short Fe–Mn bond length of 2.5393 (9) Å was observed.[4]

Table IX. ^{13}C NMR Data[a]

compd	chemical shifts[b] R group	C7,C8		C9
2a	23.1/23.7	65.4	C1,C2: 52.9	
2b	22.4/22.8; 23.3/23.6	65.4 67.8	C1: 62.9 C2: 64.2	28.8
2c	20.1; 126.9; 129.1; 135.5; 157.2		C1,C2: 71.0	
3a	23.1/23.7	65.4	C1,C2: 52.6 (t, 21 Hz)	
3b	22.5/22.9; 23.5/23.8	65.6 68.0	C1: 62.6 (t, 21 Hz) C2: 63.9 (t, 21 Hz)	29.1

[a] The values (ppm relative to TMS) have been obtained in benzene-d_6 solutions on a Bruker AC100 spectrometer using an attached proton test (t = triplet). [b] Indices according to figures 4 and 5.

The plane of the N(1)–C(7)–C(8)–N(2) skeleton, which is virtually flat, is perpendicular to the Fe–Ru bond. A similar orientation is found in $(\mu$-H)$FeMn(CO)_6(\mu,\mu'$-N-(*p*-Tol)CH_2CH_2N(*p*-Tol)). The intraligand bond lengths of 1.48 (1) Å for both C(7)–N(1) and C(8)–N(2) and 1.57 (2) Å for C(7)–C(8) are consistent with a reduction of the imine double bonds to single bonds. These distances are similar to those found in $(\mu$-H)$FeMn(CO)_6(\mu,\mu'$-N(*p*-Tol)CH_2CH_2N(*p*-Tol)).

The $M_2(CO)_6N_2$ core is typical of a broad set of compounds that can be collected into two classes: (1) those with a N–N bond, for example, in $Fe_2(CO)_6(C_{12}H_8N_2)$ with a bridging benzo(*c*)cinnoline ligand and (2) those without an N–N bond, for example, $Fe_2(CO)_6(N{=}CHCH_3)_2$ containing two bridging ethylideneamido ligands.[16a,b] The present complex **2a** obviously belongs to the second class of complexes since no N–N bond is present.

Molecular Geometry of 2b. The molecular geometry of **2b**, which is depicted in Figure 3, is almost identical with the geometrical features of **2a**. Therefore we will restrict the discussion to the main difference between **2a** and **2b**, being the presence of the methyl group C(15) attached to

(13) Dahl, L. F.; Costello, W. R.; King, R. B. *J. Am. Chem. Soc.* **1968**, *90*, 5422.

(14) (a) Busetti, V.; Granozzi, G.; Aime, S.; Gobetto, R.; Osella, D. *Organometallics* **1984**, *3*, 1510. (b) Venalainen, T.; Pakkanen, T. *J. Organomet. Chem.* **1984**, *266*, 269.

(15) For other species containing two nitrogen atoms symmetrically linking two $M(CO)_3$ units (M = Fe, Co), a bent metal–metal bond has been suggested in order to preserve the octahedral geometry of both metal atoms: Thorn, D. L.; Hoffmann, R. *Inorg. Chem.* **1978**, *14*, 126 and ref 13.

(16) (a) Gervasio, G.; Stanghellini, P. L.; Rosseti, R. *Acta Crystallogr., Sect. B: Struct. Crystallogr. Cryst. Chem.* **1981**, *B37*, 1198. (b) Doedens, R. J. *Inorg. Chem.* **1970**, *9*, 429.

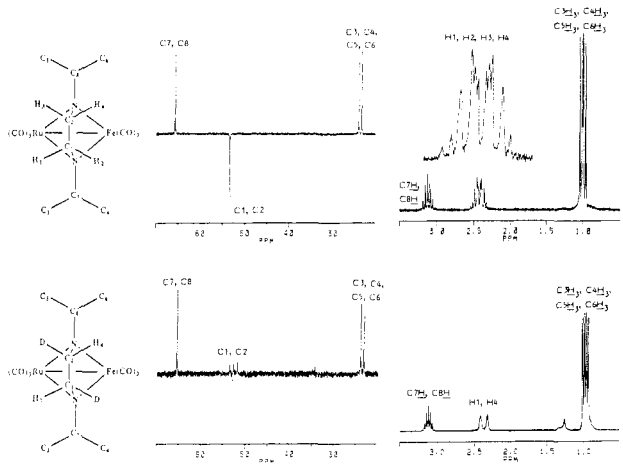

Figure 4. The schematic structures and ^{13}C NMR and ^{1}H NMR of $FeRu(\mu,\mu'$-N(*i*-Pr)CH_2CH_2N(*i*-Pr))$(CO)_6$ (**2a**) (top) and $FeRu(\mu,\mu'$-N(*i*-Pr)CHDCHCN(*i*-Pr))$(CO)_6$ (**3a**) (bottom).

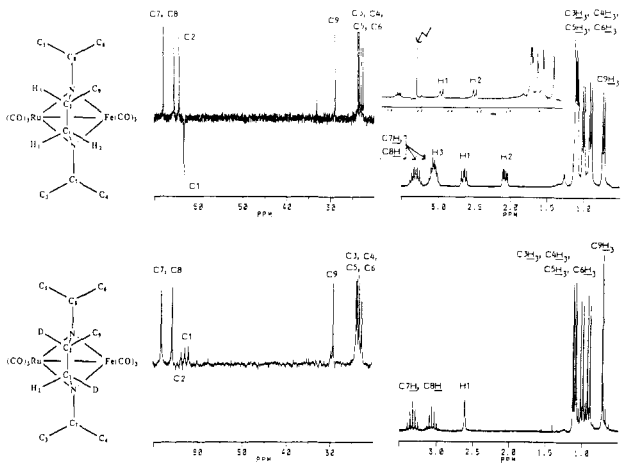

Figure 5. The schematic structures and ^{13}C NMR and ^{1}H NMR of $FeRu(\mu,\mu'$-N(*i*-Pr)CHMeCH$_2$N(*i*-Pr))$(CO)_6$ (**2b**) (top) and $FeRu(\mu,\mu'$-N(*i*-Pr)CDMeCHDN(*i*-Pr))$(CO)_6$ (**3b**) (bottom).

the ethane carbon C(7) in **2b** and consequently the different symmetry of **2a** and **2b**. The molecular structure determination revealed that the methyl group C(15) in **2b** is directed toward the iron atom in the molecule, while the molecule with this methyl group directed to the ruthenium atom is not present. As a consequence of the presence of C(15), complex **2b** possesses C_1 symmetry, compared to the C_s symmetry for **2a**. In the course of the formation of **2b** only one diasteroisomeric pair has been formed, of which the $R_{N1}R_{N2}S_{C7}$ diastereoisomer is depicted in Figure 3. Since the space group is $P2_1/n$, the $S_{N1}S_{N2}R_{C7}$ diastereoisomer is also present in the unit cell.

^{1}H and ^{13}C NMR. The ^{1}H and ^{13}C NMR data of complexes **2** and **3** are listed in Tables VIII and IX, respectively. The ^{1}H NMR and the ^{13}C NMR spectra together with schematic structures and the numbering of the atoms of complexes **2a** and **3a** are depicted in Figure 4 and those of **2b** and **3b** are shown in Figure 5. The assignment of the spectra will be discussed below.

Complex 2a. Owing to its heteronuclear character complex **2a** exhibits C_s symmetry, the mirror plane being defined by the metal atoms and the midpoint of the ethylene carbon–carbon bond, instead of C_{2v} symmetry for the related homonuclear complex. The APT ^{13}C NMR spectrum of **2a** (Figure 4, top left) shows a single negative resonance at 52.9 ppm for the equivalent secondary ethylene carbon atoms C(1) and C(2) and a single positive resonance at 65.4 ppm for both the tertiary methine carbon atoms C(7) and C(8) of the *i*-Pr groups. The primary methyl carbon atoms C(3)/C(4) and C(5)/C(6) are diastereotopic and are found as two separate, positive lines at 23.1 and 23.7 ppm. The diasterotopicity of these *i*-pR-methyl groups proves the fixed chirality of the N atoms, which is due to the presence of two different $M(CO)_3$ units in the molecule.

In the ^{1}H NMR spectrum of **2a** (Figure 4, top right) the protons of NCH_2CH_2N part of the ligand give rise to an AA'BB'multiplet centered at 2.42 ppm. Two doublets at 0.98 and 1.02 ppm for the *i*-Pr-methyl groups and one septet at 3.12 ppm for the methine protons are observed. The spectral data show that the structure in solution is the same as in the solid state (Figure 2).

Complex 3a. The APT ^{13}C NMR spectrum of the dideuteriated compound **3a** (Figure 4, bottom left) reveals the ethylene carbon atoms C(1) and C(2) as a positive triplet at 52.6 ppm. Only *one* 1:1:1 triplet is observed, proving the presence of isochronous ethylene carbon atoms which couple each with one deuterium atom, i.e. the presence of two CHD groups. From these observations it can be concluded that the reaction has resulted in the monodeuteriation of both adjacent imine carbons of the R–DAB ligand. A small negative resonance that is observed at 52.9 ppm can be assigned to a secondary ethylene carbon as in **2a**, arising from the isotopic impurity in the deuterium gas. All other resonances in the ^{13}C NMR of **3a** are identical with those observed for **2a**.

The ^{1}H NMR of **3a** (Figure 4, bottom right) shows two doublets (J(H,H) about 3 Hz) at 2.32 and 2.41 ppm, which are broadened due to deuterium coupling. This anisochronicity proves the presence of two chemically inequivalent protons in the CHDCHD fragment. All other resonances in the ^{1}H NMR of **3a** are identical with those observed for **2a**.

From these observations it follows that the deuteriation reaction of **1a** to **3a** has occurred on two different imine carbons with trans stereoselectivity (Figure 4, bottom left).

Complex 2b. Due to the methyl group $C(9)H_3$ attached to the carbon atom C(2) the molecular symmetry of **2b** is reduced to C_1 symmetry. Consequently the APT ^{13}C NMR spectrum of **2b** (Figure 5, top left) shows separate resonances for all carbon atoms. The four positive signals around 23 ppm and the two positive signals at 65.4 and 67.8 ppm can be assigned to the four primary carbon atoms C(3) to C(6) and the two tertiary carbon atoms C(7) and C(8), respectively. The carbon resonances of the C(1)C(2) fragment appears at 62.9 ppm (negative; C(1)) and 64.2 ppm (positive; C(2)), respectively, which is approximately 10 ppm downfield as compared to **2a** and **3a**. A single resonance for the primary carbon atom C(9), which is attached to the ethylene fragment, has been found as a positive signal at 28.8 ppm.[17] These ^{13}C NMR data reveal that a single isomer, in terms of disposition of the C(9) methyl group, has been formed in the hydrogenation reaction of **1a** and **2b**, which according to the X-ray structure determination of **2b** must be the isomer in which C(9) points toward the iron atom in the molecule.

The assignment of the ^{1}H NMR spectrum of **2b** (Figure 5, top right) is more complicated. For the four *i*-Pr methyl groups and the methyl group $C(9)H_3$ a total of five doublets have been observed around 0.9 ppm. From ^{1}H NMR data of the deuteriated complex **3b**, which will be discussed below, it follows that the signal at 0.72 ppm belongs to the methyl group $C(9)H_3$. Therefore the doublets at 1.10, 1.09,

(17) A relatively small resonance is observed at 32.9 ppm which is attributed to an unknown impurity.

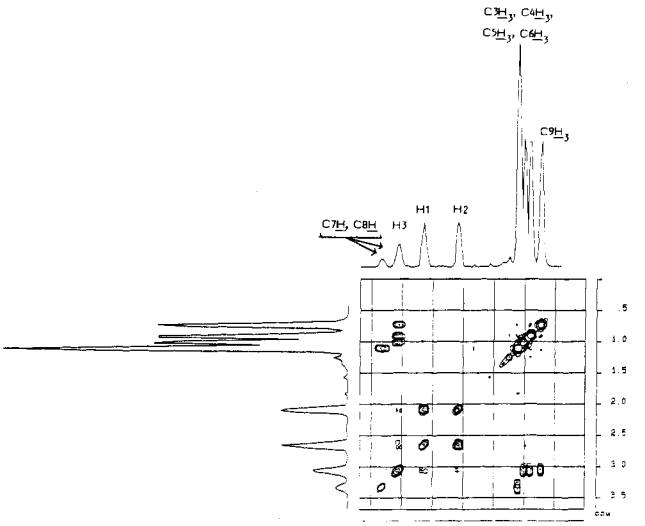

Figure 6. Homonuclear COSY NMR of FeRu(μ,μ'-N(*i*-Pr)-CHMeCH$_2$N(*i*-Pr))(CO)$_6$ (**2b**).

1.00, and 0.90 ppm belong to the four *i*-Pr methyl groups C(3)H_3, C(4)H_3, C(5)H_3 and C(6)H_3. Two septets for the *i*-Pr-methine protons C(7)*H* and C(8)*H* have been found at 3.32 and 3.09 ppm, respectively. The latter signal (integral two protons) coincides with that of one of the ethylene protons. The other two ethylene protons have been found at 2.64 and 2.07 ppm. From a homonuclear COSY spectrum (Figure 6) it appears that it is the resonance for H(3) that is buried under the septet at 3.09 ppm since there is an intense cross peak of H(3) with the C(9)H_3 protons at 0.72 ppm. No cross peak with C(9)H_3 is observed for the resonances at 2.64 and 2.07 ppm so these signals must be assigned to long-range-coupled H(1) and H(2). The resonances attributed to H(1) and H(2) show the expected strong mutual correlation in the COSY spectrum. Selective decoupling at 3.09 ppm (Figure 5, top right) indeed causes collapse of not only two *i*-Pr-Me signals associated with the septet of C(7)*H* or C(8)*H* but also collapse of the doublet of C(9)H_3 at 0.72 ppm to a singlet. Furthermore both doublets of doublets of H(1) and H(2) at 2.64 and 2.07 ppm are reduced to AB doublets with a mutual coupling of −11 Hz, which is a typical value for coupling between geminal protons. The coupling constants of H(3) in the coupled ^{1}H NMR (Figure 5, top right) with the resonances at 2.64 and 2.07 ppm amount to 7 and 5 Hz, respectively. On the basis of the Karplus–Conroy equation, the coupling of H(3) with H(1) is expected to be larger than that of H(3) with H(2) (dihedral angles of about 0° and 120°, respectively). Hence the resonance at 2.64 ppm belongs to H(1) and the signal at 2.07 ppm belongs to H(2). This assignment has been corroborated by a NOE difference experiment. A small but distinct NOE difference has been observed on the methyl resonance of C(9)H_3 at 0.72 ppm when the resonance of H(2) at 2.07 ppm was irradiated, whereas no NOE difference on C(9)H_3 was observed when the resonance of H(1) at 2.64 ppm was irradiated.

Complex 3b. In the APT ^{13}C NMR spectrum of **3b** (Figure 5, bottom left) the ethylene carbon atoms C(1) and C(2) appear at 63.9 and 62.6 ppm, respectively, as two separate triplets due to coupling of each with one deuterium nucleus. In contrast to the situation in **2b**, C(1) gives a positive and C(2) a negative signal, proving that the deuteriation reaction has occurred on the two adjacent imine carbon atoms. The other resonances are similar to that of **2b**. It may be concluded that a single diastereoisomer has been formed.

Table X. [H_2] and Temperature Dependence of the Reaction Rate with Standard Deviations in Parentheses

H_2 pressure, bar	temp, K	$[H_2]_{obsd}$, mol/L	[**1a**], mol/L	$10^{-6}k_{obsd}$, s^{-1}	$10^{-6}k$,[a] L mol^{-1} s^{-1}
20	373	0.10	0.05	35 (2)	
40	373	0.21	0.04	65 (2)	
60	373	0.32	0.05	114 (2)	353 (6)
60	383	0.32	0.10	214 (11)	696 (34)
60	393	0.30	0.10	578 (32)	1683 (107)

[a] $k = k_{obsd}/[H_2]$.

The ^{1}H NMR spectrum of **3b** (Figure 5, bottom right) shows in the ethylene region a singlet at 2.61 ppm, which is broadened due to deuterium coupling. This signal is readily assigned to H(1) as in the ^{1}H NMR of complex **2b** the resonance at 2.64 ppm has been assigned to H(1). The methyl resonance at 0.72 ppm for C(9)H_3, which was observed as a doublet in complex **2b** due to coupling with H(3), is now observed as a singlet. The signals for the ethylene protons H(2) and H(3) in complex **2b**, which were observed at 2.07 and 3.09 ppm, are obviously absent in the ^{1}H NMR spectrum of **3b**. From this observation one may conclude that H(2) and H(3) in complex **2b** are replaced by deuterium atoms in complex **3b**. It follows that the deuteriation reaction is also stereoselective and results in a mutual trans position for the deuterium atoms on adjacent carbon atoms of the ethanediyldiamido fragment. The other resonances are comparable to those in **2b**.

Monitoring the Conversion of 1a into 2a. When the reaction of **1a** to **2a** is followed with FTIR spectroscopy (ν(CO) region), one observes a smooth decrease of the absorptions due to the starting complex **1a** and a concomitant increase of the peaks of the product **2a**. The reaction was very slow below a temperature of 70 °C.

The conversion of **1a** into **2a** was followed with ^{1}H NMR using a pressurizable NMR tube.[9] As an example the spectra at t = 0, 100, 185, 290, and 370 min of the reaction at 383 K and 60 bar of hydrogen pressure are given in Figure 7. The spectrum at t = 0 shows the resonances of **1a** (*i*-Pr methyls around 1 ppm, *i*-Pr methines at 3.4 ppm, σ-N=C(H) at 7.8 ppm, and η^2-N=C(H) at 3.3 ppm), the solvent (5.3 ppm), and free hydrogen (4.6 ppm). In the next spectra at t = 100, 185, and 290 min a continuous disappearance of the resonances of **1a** is observed concomitant with the appearance of the resonances of **2a**. In the spectrum at t = 370 min **1a** is almost completely converted to **2a** (*i*-Pr methyls around 1 ppm; *i*-Pr methines at 3.1 ppm, and the ethylene protons at 2.4 ppm).

Under the conditions employed in all the reactions the hydrogen concentration is observed to be effectively constant, which can be ascribed to the diffusion of hydrogen gas from the gas phase into the solution (see Experimental Section).

Reaction Intermediates. In a search for reaction intermediates solutions of **1a** under 20 and 70 bar of hydrogen gas pressure were heated in steps of 2 K between 300 and 362 K. It was found that the reaction was negligibly slow below 343 K, at which temperature the NMR spectra indicated a slow conversion of **1a** in **2a**. Despite careful inspection of the spectra no resonances were observed that could be attributed to a steady-state buildup of an intermediate.

Kinetics of the Conversion of 1a into 2a. The kinetics of the reaction were investigated with ^{1}H NMR by monitoring the conversion of **1a** into **2a** at different hydrogen pressures and temperatures. The reaction rate for the conversion of **1a** into **2a** was observed to be first order in the concentration of **1a**, so $r = k_{obsd}$[**1a**], with rate

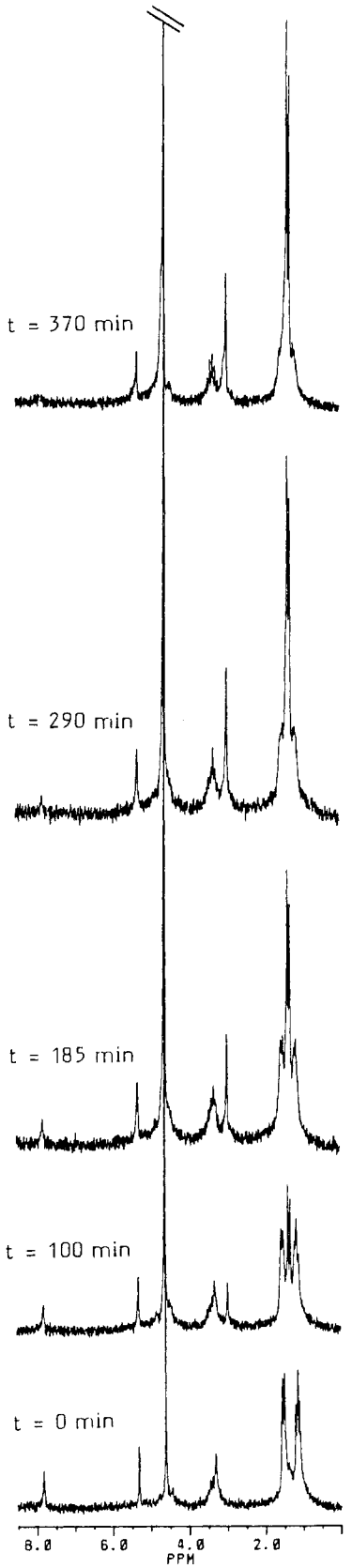

Figure 7. The conversion of $FeRu(CO)_6$(*i*-Pr-DAB(6e)) (**1a**) into $FeRu(\mu,\mu'$-N(*i*-Pr)CH_2CH_2N(*i*-Pr))$(CO)_6$ (**2a**) at 383 K at 60 bar of H_2 pressure monitored by means of ^1H NMR.

constants k_{obsd} that are compiled in Table X. The k_{obsd} values (at the fixed $[H_2]$) vary approximately proportional with the $[H_2]$ (see Table X, reactions at 373 K), confirming the first-order rate dependence on $[H_2]$. It can be concluded from the data that the reaction of **1a** with hydrogen is a second-order reaction, where $r = k[H_2][\mathbf{1a}]$, with $k = k_{obsd}/[H_2]$.

In order to determine the activation parameters of the hydrogenation, the reaction rates were measured at 373, 383, and 393 K. The second-order rate constants k at these temperatures are compiled in Table X. These data fit the Arrhenius equation and yield an E/R of 13 (3) K (or an activation energy E of 26 (6) kcal mol^{-1}).

Discussion

Reaction Mechanism. Of central interest is the mechanism of the unique hydrogenation reaction of the α-diimine ligands in complexes **1a–c**. The proposed mechanism(s) for the hydrogenation reactions should be in line with the following observations. First, the mechanism should take into account that H_2 reacts with the isoelectronic and isostructural complex $Ru_2(CO)_6$(*i*-Pr-DAB(6e)) to give *cis*-$H_2Ru_2(CO)_5$(*i*-Pr-DAB(8e)), whereas reaction of H_2 with $Fe_2(CO)_6$(*i*-Pr-DAB(6e)) leads to decomposition with the formation of unidentified products.[5a,b,18] Second, the mechanism must be in concert with the observed reaction kinetics, ie. a reaction which is first order in the concentration of both H_2 and complex **1a**, for which the kinetics were studied, and the fact that the reaction is very slow below 343 K irrespective of the applied hydrogen pressure (between 1 and 70 bar). Third, the proposed mechanism(s) must provide a good rationalization for the observed trans stereoselectivity of the hydrogenation of the central C—C bond of the N=CC=N skeleton.[19] Fourth, the mechanism should account for the observation that the Me group of the 1,2-propanediyldiamido ligand is directed exclusively to the Fe atom in complexes **2b** and **3b**. Finally, it should be noted that during the reaction the presence of a heterobimetallic pair is essential for the formation of the trans-hydrogenated (deuteriated) 1,2-ethanediyldiamido ligand.

As the deuteriation reaction of the *i*-Pr-DAB{Me,H} ligand in **1b** provides the most comprehensive information, owing to the presence of the Me group on the imine C atom, we will discuss some possible mechanisms by using **1b** as an example; see Scheme II.[20]

The first point of interest is that the reaction of $Ru_2(CO)_6$(*i*-Pr-DAB(6e)) with H_2 to give *cis*-$H_2Ru_2(CO)_5$(*i*-Pr-DAB(6e)) has been proved to proceed via the reactive intermediate $Ru_2(CO)_5$(*i*-Pr-DAB(8e)). Inspection of a model shows that the most favorable site of attack of the H_2 molecule is the void on Ru(1) of $Ru_2(CO)_5$(*i*-Pr-DAB(8e)) (Figure 1c), which does not exist on Ru(1) of $Ru_2(CO)_6$(*i*-Pr-DAB(6e)) (Figure 1b).[21] Interestingly it has been found that $Fe_2(CO)_6$(*i*-Pr-DAB(6e)) and $FeRu(CO)_6$(*i*-Pr-DAB(6e)) (**1a**) are very reluctant to form $MM'(CO)_5$(*i*-Pr-DAB(8e)) (M = M' = Fe; M = Fe, M' = Ru), although we have made many different attempts to prepare these Fe_2 and FeRu pentacarbonyl derivatives.[10]

(18) These trends are reflected when considering the reactions of $M_2(CO)_6$(R-DAB(6e)) (M = Fe, Ru) with CO. $Fe_2(CO)_6$(R-DAB(6e)) reacts with CO (1 bar, 25 °C) to give $Fe(CO)_3$(R-DAB(4e)) and $Fe(CO)_5$, whereas $Ru_2(CO)_6$(R-DAB(6e)) is stable (1 bar of CO, refluxing hexane).

(19) Hydrogenation reactions of olefins generally occur with cis stereoselectivity (see ref 23). Nonetheless the central C–C bond may have partial double-bond character in the LUMO due to π-back-bonding,[2a] so that comparison with olefins may be appropriate.

(20) It should be noted that in all the complexes **1** the imine moiety of the ligand is η^2-coordinated to Fe.

(21) The compounds $Ru_3(CO)_8$(R-DAB(8e)) and $Ru_2(CO)_5$(R-DAB(8e)), which are isolobal, possess an empty position (for $Ru_2(CO)_5$(R-DAB(8e)) the Ru(1) atom in Figure 1c). It has been observed that, e.g., CO easily attacks the empty coordination position to give $Ru_3(CO)_9$(R-DAB(8e)) and $Ru_2(CO)_6$(R-DAB(6e)), respectively. Keijsper, J.; Polm, L. H.; van Koten, G.; Vrieze, K.; Seignette, P. F. A. B.; Stam, C. H. *Inorg. Chem.* **1985**, *24*, 518 and ref 3c.

Scheme II. Suggested Mechanisms for the Formation of FeRu(μ,μ'-N(*i*-Pr)CDMeCDHN(*i*-Pr))(CO)$_6$ (3b)

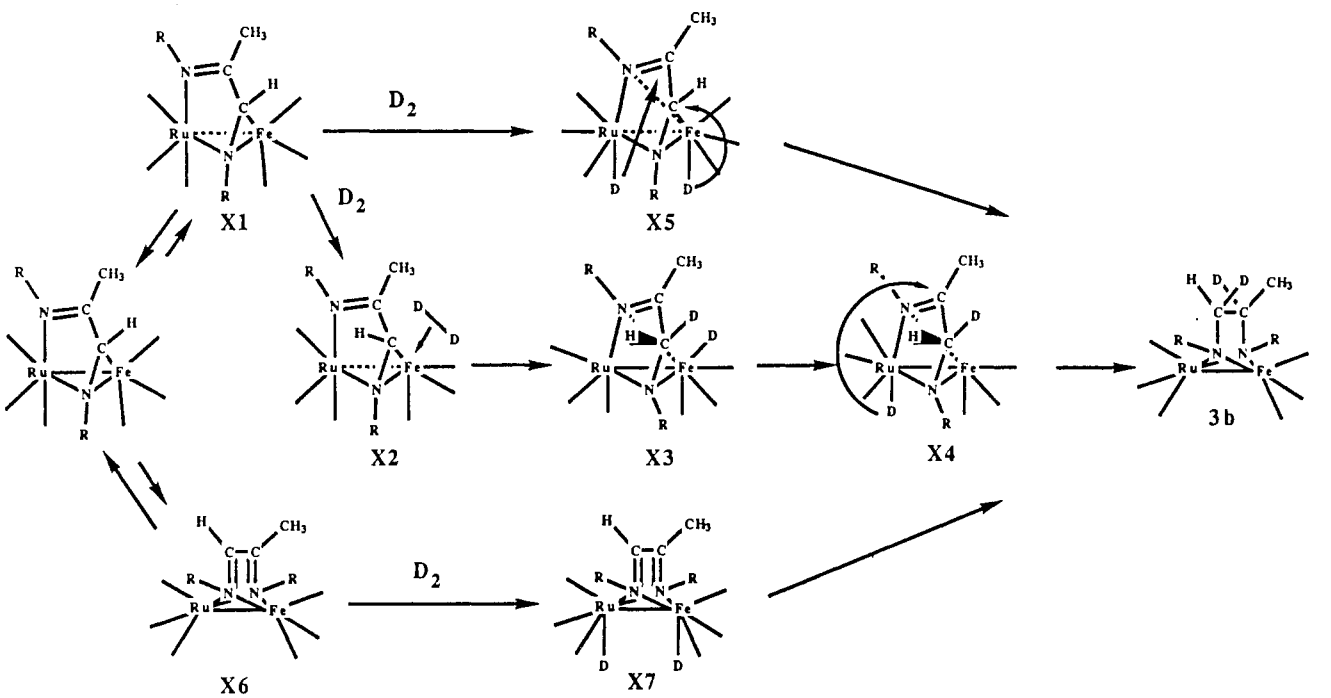

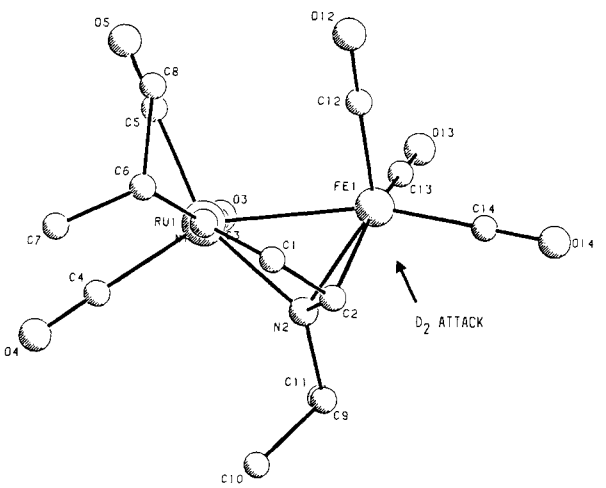

Figure 8. Molecular geometry of FeRu(CO)$_6$(*i*-Pr-DAB(6e)) (**1a**) indicating the largest void in the molecule for D_2 (or H_2) to attack.

It is therefore not surprising that the Ru atom of the mixed-metal complex **1a** is not available for attack by H_2. Nonetheless **1a** and $Fe_2(CO)_6$(*i*-Pr-DAB(6e)) do react with H_2: the Fe_2 compound decomposes no doubt due to the inherently weak Fe–Fe bond, while the FeRu compound yielded the type of complex described in this paper. It is therefore logical to search for a void on the hexacarbonyl compound **1a** suitable for attack by H_2 (D_2).[22] Such a void indeed exists on Fe in **1a** (Figure 8). This void is close to the η^2-C=N bonded imine moiety which is linked to Fe.

The observation that the reaction is very slow below 343 K at hydrogen pressures of both 1 and 70 bar indicates that the first step in the mechanism probably involves a preequilibrium between complex **1a** and a short-lived intermediate, the formation of which will be independent of the free hydrogen concentration. This equilibrium lies far to the side of **1a** since no intermediates could be observed by either NMR or FTIR experiments. The proposed preequilibrium may be represented by an equilibrium constant K (and $K = k_1/k_{-1}$).

In view of the steric arguments mentioned above it is logical to propose intermediate X1 (with a structure closely related to **1a**) as the most probable intermediate (Scheme II). In X1 the FeRu bond is ruptured, thereby creating not only a coordinatively unsaturated intermediate[23] but also a species where the void on Fe is enlarged owing to the lengthening of the FeRu distance.[24] A second, less likely, candidate for the intermediate species is X6 (Scheme II), in which the η^2-coordinated imine function has dissociated. In the unsaturated intermediate X6 the two nitrogen donor atoms may be symmetrically bridging the FeRu bond with the NCCN plane of the R-DAB ligand perpendicular to the Fe–Ru bond and the *i*-Pr-DAB{Me,H} ligand behaving as a 4e donor. An intermediate similar to X6, with two nitrogen donor atoms symmetrically bridging the metal–metal bond with the R-DAB ligand in a perpendicular fashion, has been proposed by Frühauf et al. in the photochemical rearrangement of $Fe_2(CO)_5$(P(OMe)$_3$)(R-DAB(6e)) complexes in which the η^2-coordinated imine function reversibly exchanges between the two iron atoms.[25]

The subsequent, rate-determining, step probably involves the bimolecular reaction of X1 (or less likely X6) with H_2 (or D_2 as in Scheme II), since the reaction was

(22) The complete reaction sequence will most probably proceed without CO dissociation since both complexes 1 and 2 contain six CO ligands. Even a dissociated CO group kept in the surroundings of the complex in a solvent cage is unlikely, since the reaction is performed by passing hydrogen gas through a refluxing heptane solution of complex 1. Further it is observed that the decarbonylation of **1a** on thermolysis does not proceed below a temperature of 120 °C; see ref. 10. A direct reaction of H_2 with the R-DAB ligand is unlikely since this would give cis addition; see ref 23.

(23) Kochi, J. K. *Organometallic Mechanisms and Catalysis*; Academic: New York 1978.

(24) It has been shown in previous investigations that the R-DAB ligand in the 6e coordination mode is capable to support long metal–metal distances. In $Os_3(CO)_{10}$(c-Pr-DAB(6e)) and $Ru_2(CO)_4$(*i*-Pr-DAB(6e))$_2$, which both contain 6e donating R-DAB ligands, the ligands bridge nonbonded metal–metal distances of 3.591 (3) and 3.308 (1) Å, respectively; see: Zoet, R.; Heijdenrijk, D.; Jastrzebski, J. T. B. H.; van Koten, G.; Mahabiersing, T.; Stam, C. H.; Vrieze, K. *Organometallics* **1988**, *7*, 2108 and ref 6d.

(25) Frühauf, H. F.; Meyer, D.; Breuer, J. *J. Organomet. Chem.* **1985**, *297*, 211.

found to be first order in the concentrations of complex **1a** and dissolved free hydrogen.[26] It is clear that the subsequent (hypothetical) intermediates involved in the subsequent fast steps should account for the observed stereoselectivity.

The most probable reaction route involves the intermediate X1 which reacts with D_2 to give an intermediate (η^2-D_2)FeRu(CO)$_6$(*i*-Pr-DAB;Me,H(6e)) (Scheme II, X2) in which D_2 is side-on coordinated to the Fe atom. The Fe-η^2-D_2 binding will be largely D_2-to-metal σ-donor in character, leaving the D_2 molecule with a partial positive charge.[27a-c] Since the imine carbon atom of the η^2-C(H)=N bonded moiety of the R-DAB ligand is partially negatively charged, owing to π-back-bonding from the metal into the π*-C=N orbital,[3d] it is reasonable to assume that the D_2 bond is broken and the one D atom is transferred to this imine carbon atom via a polar four-center transition state leaving the other D atom coordinated to iron (X3).[28] The D atom coordinated to Fe in X3 may now move from Fe to Ru via a bridging position giving X4 with a terminal Ru–D bond, since it is known that Ru–hydride (deuteride) bonds are more stable than Fe–hydride (deuteride) bonds. Finally the D atom on Ru will attack the imine carbon atom of the second imine group of the N=CC=N skeleton, which is now approximately perpendicular to the Fe–Ru bond, resulting in an overall trans addition of the two D atoms. This mechanism accounts for the fact that the Me group on this imine C atom must move to a position which is directed to the Fe atom and not to the Ru atom.

Less likely alternative reaction schemes involve the addition of D_2 to different metal atoms of both X1 or X6 which would lead to intermediates X5 and X7, respectively. Although species are known in which H_2 is added to two metal atoms,[29] it is more difficult to envisage such a reaction in view of steric reasons. Furthermore in a reaction route via X6 one would expect addition products with the Me group directed, on the one hand, to the Fe atom and, on the other hand, to the Ru atom in the molecule.

Finally we have excluded the possibility of a reaction involving radical species, since such a reaction would not be expected to proceed with quantitative trans addition of D_2 to the C—C bond of the N=CC=N skeleton.

Acknowledgment. We thank J. M. Ernsting for the recording of the NMR spectra, E. Kluft and G. U. A. Sai for recording the mass spectra, and Dr. H. W. Frühauf and Dr. D. J. Stufkens for stimulating discussions. We thank the Netherlands Foundation for Chemical Research (S. O.N.) and the Netherlands Organization for Pure Research (Z.W.O.) for their financial support.

Registry No. **1a**, 90219-33-3; **1b**, 117341-40-9; **1c**, 117341-41-0; **2a**, 117341-42-1; **2b**, 117341-43-2; **2c**, 117341-44-3; **3a**, 117341-45-4; **3b**, 117341-46-5; *i*-Pr-DAB, 24764-90-7; *i*-Pr-DAB{Me,H}, 78788-21-3; *p*-tol-DAB, 24764-92-9; Ru, 7440-18-8; Fe, 7439-89-6.

Supplementary Material Available: A table of elemental analysis data and tables of anisotropic thermal parameters of the non-hydrogen atoms and stereo ORTEP views for **2a** and **2b** (17 pages); listings of structure factor amplitudes for **2a** and **2b** (41 pages). Ordering information is given on any current masthead page.

(26) All reaction steps from X2 (or X7) must be fast with respect to the reaction of the intermediate X1 (or X6) with H_2 (the second-order rate constant for the reaction of X_1 (or X6) with H_2 is k; reaction rate = k [H_2][**1a**]; see results). It should further be noted that k_1 must be small compared to k_{-1} ($K = k_1/k_{-1}$ and cannot be measured) since otherwise an intermediate should have been observed.

(27) (a) Crabtree, R. H. *Inorg. Chim. Acta* **1986**, *125*, L7. (b) Crabtree, R. H.; Lavin, M. *J. Chem. Soc., Chem. Commun.* **1985**, 794. (c) Crabtree, R. H.; Hamilton, D. G. *J. Am. Chem. Soc.* **1986**, *108*, 3124.

(28) An example of hydrogen transfer from a metal to an imine carbon atom is the reaction of $HRu_3(\mu$-NC(H)(Ph))$(CO)_{10}$ with H_2 to $HRu_3(\mu$-N(H)CH_2Ph)$(CO)_{10}$ Bernhardt, W.; von Schnering, C.; Vahrenkamp, H. *Angew. Chem., (Int. Ed. Engl.)* **1986**, *25*, 279.

(29) Examples are: (i) [Ir(μ-S-*t*-Bu)(CO)(PPh_3)]$_2$ reacts with H_2 to [IrH(μ-S-*t*-Bu)(CO)(PPh_3)]$_2$ which lacks an Ir–Ir bond and has one hydrogen atom coordinated to each Ir atom: Bonnet, J. J.; Maissonnat, T. A.; Galy, J.; Poilblanc, R. *J. Am. Chem. Soc.* **1979**, *101*, 5940. (ii) [(MeCp)Mn$(CO)_2(\mu$-*t*-Bu_2P)Ir(COD)] reacts with H_2 by cleavage of the Mn–Ir bond to [(MeCp)Mn$(CO)_2(\mu$-*t*-Bu_2PH)]: Arrif, A. M.; Chandler, D. J.; Jones, R. A. *Inorg. Chem.* **1987**, *26*, 1780. (iii) [FeIr(μ-PPh_2)$(CO)_5(PPh_3)_2$] reacts with H_2 by cleavage of the Fe–Ir bond to [$FeIrH_2(\mu$-PPh_2)$(CO)_5(PPh_3)_2$] in which the H_2 is oxidatively added to the Ir atom: Roberts, P. A.; Steinmetz, G. R.; Geoffroy, G. L. *Organometallics* **1983**, *2*, 846.